

Unbiased Cold Denaturation: Low- and High-Temperature Unfolding of Yeast Frataxin under Physiological Conditions

Annalisa Pastore,[†] Stephen R. Martin,[†] Anastasia Politou,[‡] Kalyan C. Kondapalli,[§]
Timothy Stemmler,[§] and Piero A. Temussi^{*,†,#}

National Institute for Medical Research, Medical Research Council, London U.K., Medical School, University of Ioannina, Ioannina 45110, Greece, Department of Biochemistry and Molecular Biology, School of Medicine, Wayne State University, Detroit, Michigan, and Department of Chemistry, Università di Napoli Federico II, via Cinthia, 80126 Napoli, Italy

Received March 1, 2007; E-mail: temussi@unina.it

Protein unfolding can be induced both by heating and by cooling from ambient temperatures.¹ Accurate analysis of heat and cold denaturation processes has the potential to unveil hitherto obscure aspects of protein stability and dynamics.² For instance, while heat denaturation is generally highly cooperative, cold denaturation has been suggested to occur in a non-cooperative fashion.^{3,4} This view has been recently supported by an NMR study of ubiquitin in reverse micelles at very low temperatures,⁵ but this is still controversial since Van Horn et al.,⁶ on the basis of similar NMR data, and Kitahara et al.,⁷ by an NMR study at 2 kbar, found a simple two-state behavior for the low-temperature unfolding of ubiquitin.

To reach a consensus on this debate and other general issues, it is necessary to investigate cold denaturation further. However, since the cold denaturation of most proteins occurs well below the freezing point of water, full access to the cold denatured state is normally limited for the obvious reason that water freezes at 0 °C. The most common approach to circumvent this difficulty has been to try to raise the temperature of cold denaturation using destabilizing agents such as extreme pH values, chemical denaturants, cryosolvents, or very high pressure.^{7–10} Alternatively, some laboratories used proteins destabilized by a combination of point mutations and denaturing agents.⁹ The main drawback of these approaches is that it is not generally easy to extrapolate results to physiological conditions. On the other hand, there are methods aimed at keeping water in a supercooled condition, but these studies have also invariably used destabilized proteins.^{11,12}

Following a different approach, we looked for a protein whose cold denaturation could be studied without the need for destabilization in a normal buffer at physiological pH within a temperature range accessible to several techniques. Here we describe the cold and heat denaturation of yeast frataxin (Yfh1) measured both by NMR and CD spectroscopies. In a systematic study of the factors that influence the thermal stability of the frataxin fold, we had previously shown that although they share the same fold, three orthologues from *E. coli* (CyaY), *S. cerevisiae* (Yfh1) and *H. sapiens* (hfra), are characterized, under the same conditions, by a remarkable variation of melting temperatures.¹³ Yfh1, the one with lowest heat denaturation temperature, seemed a promising candidate for cold denaturation above 0 °C. Yfh1 and ¹⁵N-labeled Yfh1 were expressed in *E. coli* as described by He et al.¹⁴ Since variations of ionic strength lead to significant increases in the melting temperature, we restricted the present investigation to solutions of Yfh1 in salt-free buffers.

We recorded 1D and 2D NMR spectra of Yfh1 either in TRIS at pH 7.0 or in HEPES at pH 7.0 in the temperature range –5 to 45 °C. Typically, 0.3–0.5 mM unlabeled or ¹⁵N uniformly labeled protein samples were used. Thanks to the vibration-free environment afforded by NMR spectrometers, it proved easy to keep the solutions even below 0 °C for extended periods. NMR spectra were recorded on a Varian INOVA spectrometer operating at 600 MHz ¹H frequency.

Figure 1A shows the comparison of the ¹⁵N-¹H HSQC correlation spectrum of Yfh1 in 20 mM HEPES at 20 °C with the corresponding spectra at the two extremes of the temperature range. Spectra at –5 and 45 °C are collapsed, in agreement with a completely unfolded state. The small differences can be easily accounted for by the different exchange rates of the amide protons at different temperatures.

The 1D regions of Figure 1B show the concomitant change of several ring current shifted resonances, arising from aliphatic groups close to aromatic rings in the hydrophobic core of the protein. Changes in their relative intensity can be directly linked to changes of the tertiary structure of the protein. Several high-field peaks were accurately integrated and calibrated with respect to a standard reference peak. Integrals were then normalized for each peak using the highest measured value.

Figure 2 (right y-axis) shows the plot of the integrals of four well-separated high-field peaks, that is, those marked as a, b, c, and d in Figure 1 as a function of temperature. All points fall on the same curve, consistent with a low-temperature transition at ca. 7 °C and a high-temperature transition at ca. 31 °C. To further validate these findings we used CD measurements.

Far-UV CD measurements were made using a Jasco J-715 spectropolarimeter equipped with a PTC-348WI Peltier temperature controller. Thermal unfolding curves were obtained by monitoring ellipticity at 222 nm using 2 mm path-length cuvettes and a heating rate of 1 °C/min (Figure 2, left y-axis). The CD curve in HEPES is essentially superimposable to that recorded in TRIS (data not shown).

For a simple two state equilibrium between folded and unfolded forms of a protein of the size of frataxin, the fraction of protein present in the folded form at any temperature, $f_F(T)$, is a function of $\Delta G^\circ(T)$, the Gibbs free energy for unfolding. If the heat capacity difference between the folded and unfolded forms, ΔC_p , is independent of temperature, the free energy is given by the Gibbs–Helmholtz equation modified so that the reference temperature is the midpoint of the high-temperature transition (T_H).¹ A nonlinear least-squares fit to the observed $f_F(T)$ values then allows one to determine T_H , $\Delta H^\circ(T_H)$, and ΔC_p . The corresponding values for low-temperature unfolding (T_L and $\Delta H^\circ(T_L)$), can then be deter-

[†] National Institute for Medical Research.

[‡] University of Ioannina.

[§] Wayne State University.

[#] Università di Napoli Federico II.

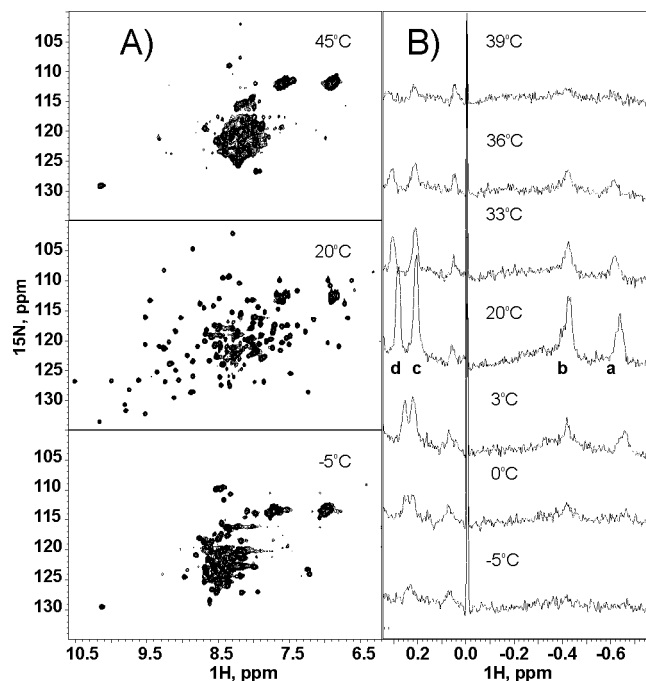


Figure 1. Representative NMR spectra of Yfh1 in the temperature range -5 to 45 °C: (A) ^{15}N - ^1H HSQC correlation spectra of Yfh1 in 20 mM HEPES at pH 7.0 at three representative temperatures; (B) high field portions of 1D spectra of Yfh1 in 20 mM HEPES at pH 7.0 at seven representative temperatures. The sample used for quantitative measurements was extensively dialyzed and contains TSP for reference (0 ppm) and calibration.

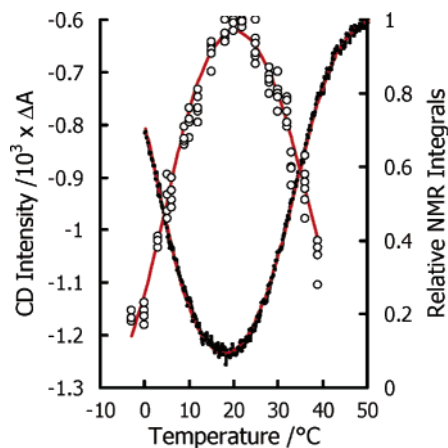


Figure 2. Plots of NMR and CD signals of Yfh1 as a function of temperature. Relative integrals of the highest field peaks of Yfh1 in HEPES at pH 7.0 are shown as circles (right-hand side scale). Far UV absorbance in the CD spectra of Yfh1 in 20 mM Tris at pH 7.5 corresponds to the left-hand side scale.

mined from a plot of ΔG° against temperature.¹² Values of the entropy change at T_L and T_H can be obtained from the relationship $\Delta G^\circ = \Delta H^\circ - T\Delta S^\circ$. In principle, the f_F values can be calculated by dividing the difference between the observed CD or NMR signal and the signal of the unfolded state by the difference between the signals of the folded and unfolded forms. However, since there is no distinguishable plateau between the two transitions, in the data fitting analysis it was necessary to vary the signal for the fully folded protein to get the best fit to $f_F(T)$.¹² Once this value is

Table 1. Thermodynamic Parameters Averaged over NMR and CD Data

	low melting	high melting
$T/^\circ\text{C}$	7 ± 1.5	30.5 ± 2
$\Delta H^\circ/\text{kJ mol}^{-1}$	-85 ± 10	89.5 ± 8
$\Delta S^\circ/\text{J mol}^{-1} \text{K}^{-1}$	-305 ± 35	295 ± 25
$\Delta C_p/\text{kJ mol}^{-1} \text{K}^{-1}$	7.57 ± 0.15	7.57 ± 0.15

determined, a back calculation yields a figure of $\sim 67\%$ for the fraction folded at the temperature of maximum stability.

Table 1 summarizes the thermodynamic parameters of this analysis. It can be appreciated that since both NMR and CD data were fit by the same equation (red lines in Figure 2), it is possible to say that the disruption of the hydrophobic core is exactly paralleled by a decrease of the secondary structure content. As expected, cold denaturation has “thermodynamic anomalies”: both ΔH and ΔS are large and negative for this transition.

We have shown that a protein with a native low stability, can undergo a low-temperature melting without the need of destabilizing it by chemical or physical means or by introducing arbitrary point mutations. Yfh1 is an excellent model system to study low- and high-temperature transitions in a range accessible to many techniques, and thus it promises to reveal new insights on the influence of several parameters on protein unfolding. For instance, although it has been postulated that the effect of hydration entropy can be intrinsically different for cold and heat denaturation,¹⁵ it is generally difficult to detect such an asymmetry experimentally. Thanks to the short range in which the two transitions occur for Yfh1, we can expect that even small variations in environmental parameters can reveal differential effects on the two transitions.

Acknowledgment. Financial support from an International JOINT PROJECT of the Royal Society (NIMR: U.1175.03.002.-00010.01) to A.P. and P.A.T. and from MIUR (FIRB 2003) to P.A.T. are gratefully acknowledged. Support for T.L.S. comes from the NIDDKD (Grant R01 DK068139) and for K.C.K. from the American Heart Association (Grant 0610139Z).

References

- (1) Privalov, P. L. *Crit. Rev. Biochem. Mol. Biol.* **1990**, *25*, 281–305.
- (2) Caldarelli, G.; De Los Rios, P. *J. Biol. Phys.* **2001**, *27*, 229–241.
- (3) Freire, E.; Murphy, K. P.; Sanchezruiz, J. M.; Galisteo, M. L.; Privalov, P. L. *Biochemistry* **1992**, *31*, 250–256.
- (4) Griko, Y. V.; Venyaminov, S. Y.; Privalov, P. L. *FEBS Lett.* **1989**, *244*, 276–278.
- (5) Whitten, S. T.; Kurtz, A. J.; Pometun, M. S.; Wand, A. J.; Hilser, V. J. *Biochemistry* **2006**, *45*, 10163–10174.
- (6) Van Horn, W. D.; Simorellis, A. K.; Flynn, P. F. *J. Am. Chem. Soc.* **2005**, *127*, 13553–13560.
- (7) Kitahara, R.; Okuno, A.; Kato, M.; Taniguchi, Y.; Yokoyama, S.; Akasaka, K. *Magn. Reson. Chem.* **2006**, *44*, S108–S113.
- (8) Griko, Y. U.; Privalov, P. L.; Sturtevant, J. M.; Venyaminov, S. Yu. *Proc. Natl. Acad. Sci. U.S.A.* **1988**, *85*, 3343–3347.
- (9) Chen, B.; Schellman, J. *Biochemistry* **1989**, *28*, 685–699.
- (10) Jonas, J. *Biochim. Biophys. Acta* **2002**, *1595*, 145–159.
- (11) Babu, C. R.; Hilser, V. J.; Wand, A. J. *Nat. Struct. Mol. Biol.* **2004**, *11*, 352–357.
- (12) Szyperki, T.; Mills, J. L.; Perl, D.; Balbach, J. *Eur. Biophys. J.* **2006**, *35*, 363–366.
- (13) Adinolfi, S.; Trifuoggi, M.; Politou, A. S.; Martin, S.; Pastore, A. *Hum. Mol. Genet.* **2002**, *11*, 1865–1877.
- (14) He, Y.; Alam, S. L.; Proteasa, S. V.; Zhang, Y.; Lesuisse, E.; Dancis, A.; Stemmler, T. L. *Biochemistry* **2004**, *43*, 16254–16262.
- (15) Privalov, P. L.; Makhatadze, G. I. *J. Mol. Biol.* **1993**, *232*, 660–679.

JA0714538